Corrosion Properties of 70 Sio_2-15Tio_2-15Zro_2 Ceramic Membrane

M. Shojaie Bahaabad[a], E. Taheri Nasaj[a,]*, K. Falamaki[b], A. Zakeri[c]

[a] *Department of Materials Engineering, Tarbiat Modares University, Tehran, Iran.*
[b] *Department of Chemical Engineering, Amirkabir University, Tehran, Iran.*
[c] *Sarkhoon and Qeshm Gas Treating Company, Bandar Abbas, Iran.*

ARTICLE INFO

Article history:

Received 15 March 2014
Accepted 16 May 2014
Available online 31 Aug. 2014

Keywords:

Ceramic membrane
Corrosion
Chemical stability
SiO_2 membrane

ABSTRACT

The $70SiO_2$-$15TiO_2$-$15ZrO_2$ membrane was prepared by a sol-gel procedure. Corrosion behavior of the microporous top layer along with the membrane characterization in terms of pore size, surface area, pore volume and weight loss are described. The final ceramic membrane with a thickness of 400 nm and uniform surface was obtained. This membrane confirmed the fine microporous characteristic with mean pore size < 2 nm. After corrosion test, the corroded membrane revealed a surface with non-uniform coverage of the top layer. The heated ceramic membrane was amorphous before and after corrosion test. Dissolution of ions increased in acid and basic solutions. The weight loss of samples increased when pH increased at 25 °C. Porosity of samples increased after the corrosion test. The pore size increased as compared to that of the original membrane. Surface area of the membrane increased in basic solution, but decreased in acid solution.

1. Introduction

Nanofiltration (NF) membranes are generally classified into two major groups: organic polymeric and inorganic ceramic membranes. Polymeric membranes constitute the most important group and have been commercially available for many years. They are relatively easy to prepare and can be produced cheaply at large scale. However, their application is limited to moderate temperatures and to feed streams which are not too corrosive [1]. Ceramic membranes generally possess a high thermal, chemical and mechanical stability. Nonetheless, they are less frequently considered for NF applications, because their fabrication is often more complex and, hence, more costly [2, 3]. Main advantages of ceramic membranes include: (1) resistance against dissolution and swelling upon exposure to organic solvents; (2) ability to withstand high temperatures; (3) ability of exposure towards extreme pH values; (4) long service-life [4, 5]. Materials considered for mesoporous and microporous membrane formation include: α-Al_2O_3, TiO_2, ZrO_2, and SiO_2. Of these, α-Al_2O_3 and SiO_2 are suitable for application in organic liquids, but these materials do not display high enough chemical stability at high and low pH values [6]. Some researcher reported acid corrosion tests on mesoporous ceramic alumina, titania and zirconia membrane. Measurements of membrane corrosion showed that titania and zirconia membrane were more stable than alumina membrane. Unfortunately,

Corresponding author:
E-mail address: Taheri@modares.ac.ir (Ehsan Taheri Nassaj).

investigations on membrane retention characteristics are lacking and only a relatively short exposure time of 16 hr was applied. These researchers reported briefly dynamic corrosion tests on mesoporous alumina membrane. They investigated the corrosion of micro and mesoporous alumina, alumina-titania, and titania NF membrane materials in acid and alkaline solutions. They indicated the important material parameters like the phase structure and the presence of amorphous phases. Mesoporous gamma alumina showed a high corrosion in strong acid and alkaline solutions; for micro and mesoporous anatase phases a low corrosion was found [5, 6]. Remarkably, the stability of ceramic NF membranes in aqueous corrosive liquids, like strong acid and alkaline solutions, has not been investigated yet. As a consequence, experimental corrosion data and well-defined measuring methods for evaluation of membrane corrosion are lacking [7]. Measurements of membrane corrosion based on changes in permeability or analysis of dissolved ions is a way that shows membranes are stable in corrosion conditions or not [8]. Moreover, at present only limited data are available on the corrosion behavior of the silica ceramic membrane materials. Amorphous silica, which is an acid metal oxide, is not stable in aqueous solutions, especially in neutral and alkaline solutions, but has a great advantage in terms of pore size controllability. Therefore, incorporation of other components such as zirconium, aluminium and nickel into silica has been investigated [8].

Ceramic NF-membranes with high performance parameters such as high fluxes can only be obtained in an asymmetric multilayer configuration. The development of such a multilayer configuration includes: shaping of an appropriate support material; formation of mesoporous interlayers; and synthesis of a microporous top layer. Alumina, titania, zirconia or silica are considered as the main ceramic materials for the formation of the multilayer structures [9-11].

The preparation route starts with the production of a high-quality support system, as the effectiveness of the developed NF membrane is greatly influenced by the structural properties of the membrane support. In this study, alumina supports were produced by conventional pressing. The second stage involves the synthesis of several intermediate membrane layers. The aim of this modification is twofold: fine-grained mesoporous membrane layers are necessary in order to reduce the coarse pore structure of the support material and large surface irregularities or defects can only be covered properly by a multiple dip-coating procedure [12]. In this study, colloidal sol-gel derived membrane layer consisting of titania is considered. The final step in the multilayer preparation route involves the synthesis of a thin separation top layer. Formation of such a layer with very small pores requires an appropriate sol consisting of very small nanometer-sized particles, which is typically obtained by the so-called 'polymeric' sol-gel technique. In this work, $70SiO_2$-$15TiO_2$-$15ZrO_2$ top layer is formed by polymeric sol-gel procedure. Fig 1 shows an asymmetric ceramic multilayer membrane.

The aim of this paper is to provide results on the chemical stability of the sol-gel derived $70SiO_2$-$15TiO_2$-$15ZrO_2$ membrane. The corrosion behavior of the microporous top layer along with the membrane characterization in terms of pore size, surface area, pore volume and weight loss is described. For determination of the corrosion rate, preference was given to simple static corrosion experiments whereby the amount of dissolved membrane material was determined in acid or alkaline solutions. The performance surface characteristics of the multilayer membranes are also described to indicate the possible application fields of the developed NF-membranes.

2. Experimental

2. 1. Membrane preparation

2. 1. 1. Preparation of the support material

Al_2O_3 supports were prepared by α-Al_2O_3 powder (particle: 0.3 μm, surface area: 6 m^2/g) with organic additives (CMC). After shaping of the support material by pressing, heat treatment was performed at 1420 ºC for 2 hours. The final support discs were 20 mm in diameter and 2 mm in thickness.

2. 1. 2. Preparation of the membrane interlayer by colloidal sol-gel process

The precursors for colloidal sol-gel process were common titanium based organometallic

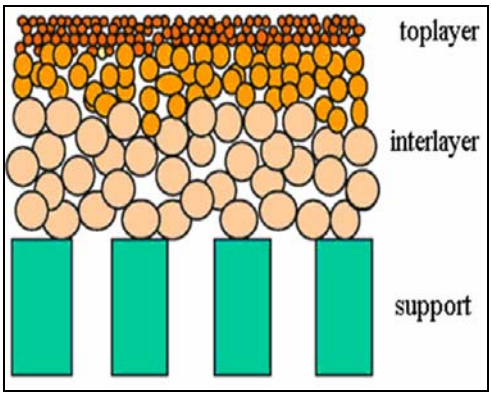

Fig. 1. Schematic of an asymmetric ceramic multilayer membrane

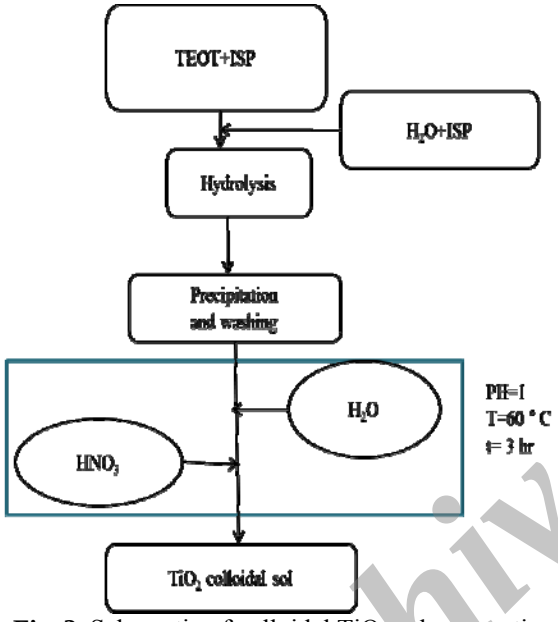

Fig. 2. Schematic of colloidal TiO_2 sol preparation

compounds, which were hydrolyzed by addition of an excess H_2O. The TiO_2 sol was obtained by hydrolysis of tetraethyl orthotitanate (TEOT, 8218950, Merck) by isopropanol (ISP, 38122334, Merck), distilled water and nitric acid (65%, 100456, Merck). The procedure of sol preparation is shown in Fig 2.

For preparation of titania membranes, a solution of hydroxypropyl cellulose (HPC, 4355007, Aldrich) with MW= 100,000 (1 g/100 ml H_2O) and PVA (821038, Acros) with MW= 72,000 (3.5 g/100 ml H_2O)) was added as drying chemical controlling additive (DCCA) to the sols before membrane formation. Supported gel layers were formed on the membrane support by dip-coating the supports with freshly prepared sols. Non-supported gel layers were produced by pouring the remaining sol-gel solutions in petri-dishes. Afterward, they were dried for 72 hours in 80% humidity at 30 ºC. The coating and the powder were heat treated at 500 ºC and heating rate of 5 ºC/min and then kept in this temperature for 1 hour.

2. 1. 3. Preparation of the membrane top layer by polymeric sol-gel process

A polymeric $70SiO_2$-$15TiO_2$-$15ZrO_2$ sol was produced starting from tetraethyl orthosilicate (TEOS, 493958748, Merck), titanium isopropoxide (TTIP, 4707295, Merck), zirconium isopropoxide (96595, Fluka), 2-methoxy-4-propenylphenol (isoH, 818455, Merck), nitric acid (65%, 100456, Merck), and ethanol (EtOH, 38913389828, Merck). The procedure of sol preparation is shown in Fig 3. The molar ratios TEOS:EtOH:H_2O:HNO_3 were 1:3.8:1:0.06 in SiO_2 sol. For preparation of Ti and Zr sol, the molar ratio isoH/(Zr,Ti) , isoH/EtOH and (Zr,Ti)/EtOH were 2,0.1,0.02, respectively. In contrast with the colloidal route, for preparation of very fine polymeric membrane layer no high molecular weight organic additives could be added. Therefore, the freshly prepared $70SiO_2$-$15TiO_2$-$15ZrO_2$ sol was aged for 3 days in order to increase the viscosity of the dipping solution and to prevent penetration of the sol into the pores of the intermediate support layer during dip-coating. At the same time, unsupported membranes were prepared by evaporating the sol in a petri-dish. Heat treatment was performed at the same procedure used for interlayer preparation.

2. 2. Characterization

2. 2. 1. Static characterization

Several methods were used for characterization of the membrane support. The structure was analyzed by X-ray diffraction (XRD, Philips-Xpert) and Hg-Porosimetry (Autoscan-33, Porosimeter, Quantachrome). The pore size and the presence of possible defects in the supports were determined by field emission scanning electron microscopy (FESEM, TESCAN-MIRAS). Surface roughness was measured with a laser profilometer (Micro Focus Measurement System, UBM). Mechanical properties were characterized by four-point

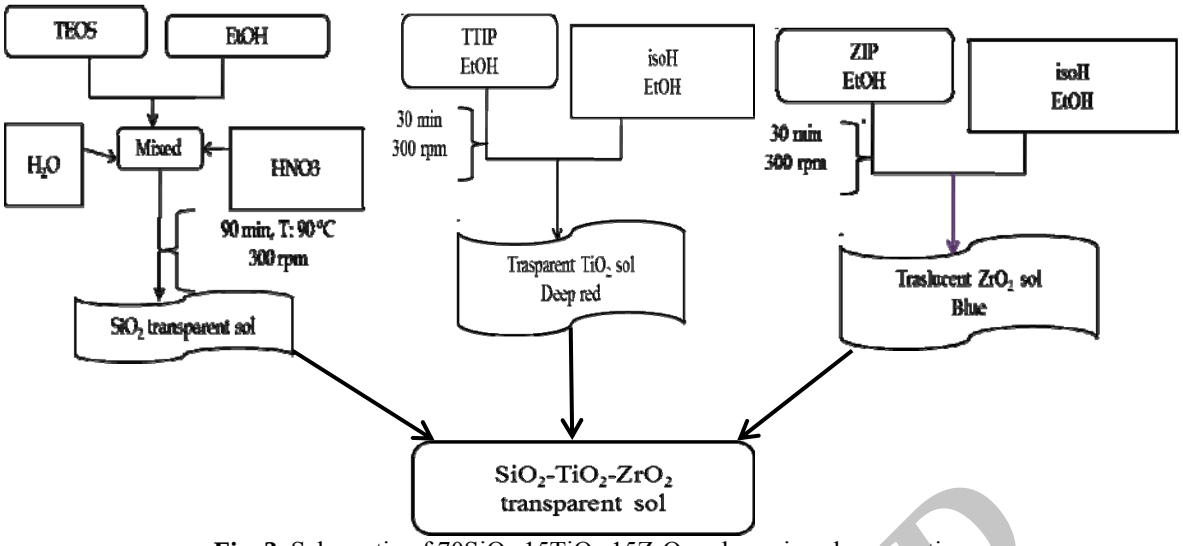

Fig. 3. Schematic of $70SiO_2$-$15TiO_2$-$15ZrO_2$ polymeric sol preparation

Table 1. Characteristics of the support material

Thermal treatment (ºC)	Phase	Pore size (µm)	Porosity (%)	Roughness (µm)	Bend-strength (MPa)	Corrosion pH=1 (µg Al/l)
1420	α-Al_2O_3	300	35%	1.22	43	-

bend tests (Chevron-notch). The particle sizes in sol were determined by the Dynamic Laser Beam Scattering technique (DLS, Malvern). Morphology, surface quality, and thickness of the interlayer and top layer were examined by field emission scanning electron microscopy (FESEM, TESCAN-MIRAS). XRD measurements were used for determination of the phase composition in the membrane material. N_2-adsorption/desorption measurements were performed to determine the pore size distribution, surface area, and pore volume. All structural measurements were carried out on unsupported membrane interlayers and top layers, assuming that their properties were similar to those of supported membrane layers.

2. 2. 2. Static corrosion test

Static corrosion tests were performed in aqueous solutions at pH=1, 3. These solutions were prepared using demineralized water and nitric acid (Merck, pro analysis ([Al]= 0.05 ppm, [Ti]= 0.02 ppm)). Then, 100 mg of calcined membrane material was immersed in 100 ml of the acid solution. After the exposure time, liquid samples were taken, filtered over a Whatman 42 filter and analyzed for their Si, Zr and Ti concentration by inductively 0.1 coupled plasma-mass spectroscopy (VG-PlasmaQuad PQ-2 Plus). After filtering, the calcined membrane material powder was collected and dried at 200 ºC for 2 hours. Weight loss was calculated by comparing the powder sample weight before and after corrosion test. Additionally, corrosion experiments were conducted in $NaOH_4$ solutions (Merck, (Al content = 0.0005%)) at pH=9,11. All corrosion experiments were performed at 25 ºC. The pH measurements were carried out with a digital pH-meter (ATI Orion 310).

3. Results and Discussion

3. 1. The support material

For development of high-quality supports the following properties are of major importance: pore size distribution, porosity, surface quality with the absence of large defects or large pores, and mechanical and chemical stability. Structural characteristics of the final Al_2O_3 membrane support are summarized in Table 1.

Long term corrosion measurements on α-Al_2O_3 support material in nitric acid solutions also showed a high chemical stability. For a corrosion test at pH=1, only small amounts of

Table 2. Experimental conditions for preparation of the stable sols

Stable sols	$[H_2O]/[M]^a$	$[HNO_3]/[M]^a$	isoH/(Zr,Ti)	isoH/EtOH	(Zr,Ti)/EtOH	pH	Temperature (ºC)	Particle size (nm)	Characteristics
TiO_2[b]	25	0.5	-	-	-	1	70	35	Opaque blue
SiO_2-TiO_2-ZrO_2[C]	0.4	0.04	2	0.1	0.02	5.55	RT	8	Transparent deep red

[a] [M] = [TEOT], [TTIP], [ZIP]
[b] Colloidal sol
[c] Polymeric sol

aluminum were found even after an exposure time of 6 months.

3. 2. Sols

Both the colloidal and the polymeric sols were prepared by hydrolysis of alkoxide precursors to induce condensation and inorganic polymerization reactions. For the formation of mesoporous membrane interlayers, suspensions of relatively large nanometer-sized particles were needed. This was obtained by reacting the alkoxide precursors with a large excess water ($[H_2O]/[TTI] > 4$), followed by a refluxing step overnight under the conditions shown in Table 2.

The final products after peptization were stable fine colloidal sols. According to PCS measurements, TiO_2 sol consisted of cylindrical particles with a mean size of about 35 nm. Due to the presence of relatively large particles, these sols were semi-transparent and looked light blue. For synthesis of the $70SiO_2$-$15TiO_2$-$15ZrO_2$ top layer, a precipitate free sol containing small nanometer-sized polymeric structures (fractals) was prepared. The essential features of the polymeric sol preparation were a carefully controlled hydrolysis with a less than stoichiometric amount of water ($[H_2O]/[Ti/Zr] < 4$) followed by an appropriate aging. The final aged polymeric sol was completely transparent.

3. 3. Membrane interlayer

3. 3. 1. Morphology

For development of high-quality multilayer membrane, we aimed at the formation of rather thick intermediate layer, which was required to overcome inevitable surface irregularities of the support. In practice, in all membrane formation procedures a second dip-coating step was used after calcination of the first layer. This was done to repair defects such as pinholes or regions with non-uniform layer formation, which often appeared in the first sol-gel intermediate layer. Each final support thus produced consisted of the main support with two sol-gel derived membrane layers. Therefore, a second dipping procedure was required to increase the membrane thickness up to 4.6μm (Fig 4).

3. 3. 2. Structural properties

After thermal treatment at 500 ◦C, titania membrane appeared in the crystallographic anatase phase (Fig 5). The shape of the adsorption/desorption isotherms was characterized as type IV (Fig 6), which confirmed the fine mesoporous characteristic of this membrane material with the mean pore size 5 nm, surface area 135 m^2/g, and pore volume 0.14 cm^3/g.

3. 4. Membrane top layer

3. 4. 1. Morphology

The finally obtained ceramic membranes can be categorized as typical asymmetric multilayer membranes. Fig 7 shows the surface and cross-section of a polymeric sol-gel derived ceramic top layer with a thickness of 400 nm. It appears that uniform and discrete layers were formed and penetration of the top layer into the

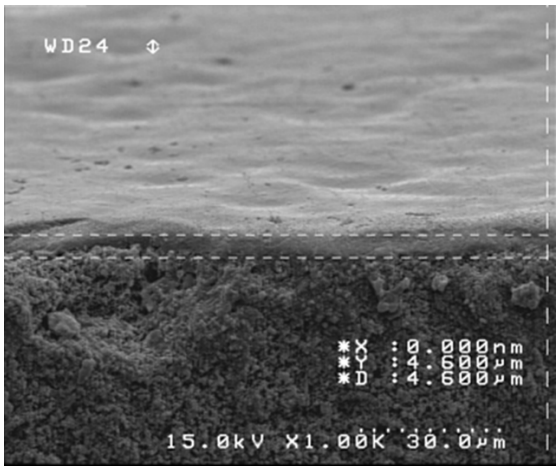

Fig. 4. FESEM cross-section of titania colloidal sol-gel membrane layer on α-Al_2O_3 heated at 500 ºC for 1 hour

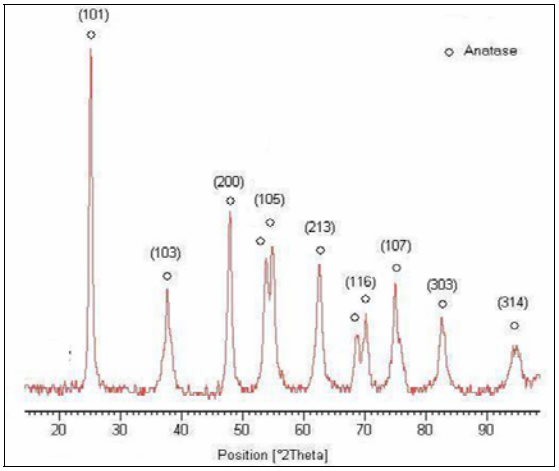

Fig. 5. XRD pattern of titania ineterlayer membrane heated at 500 ºC for 1 hour

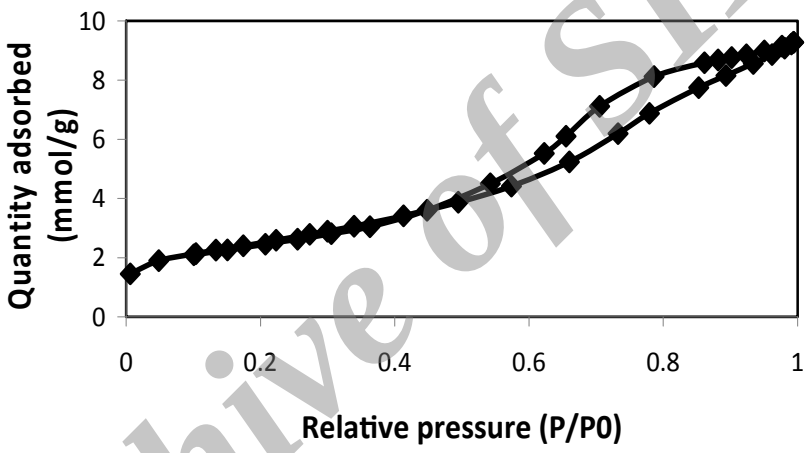

Fig. 6. N_2 adsorption/desorption of titania ineterlayer membrane heated at 500 ºC for 1 hour

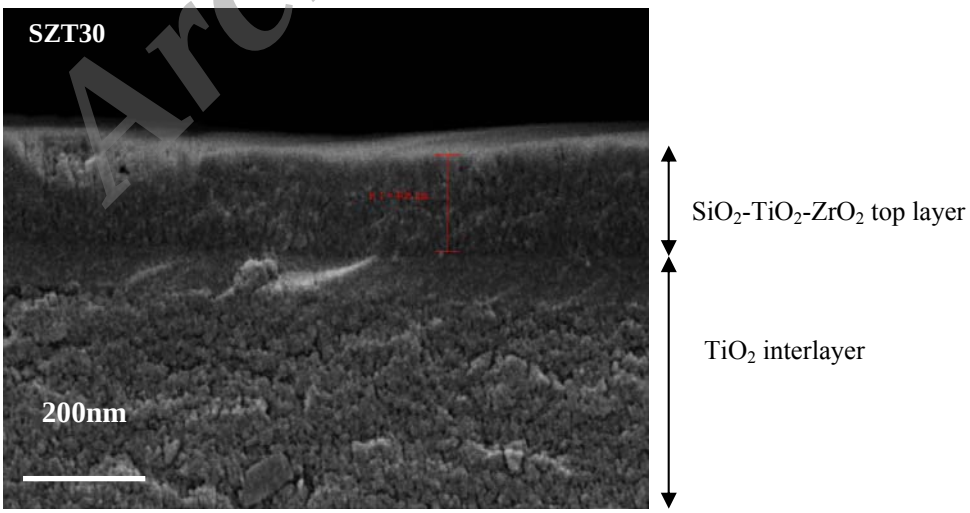

Fig. 7. FESEM cross-section of a multilayer membrane heated at 500 ºC for 1 hour

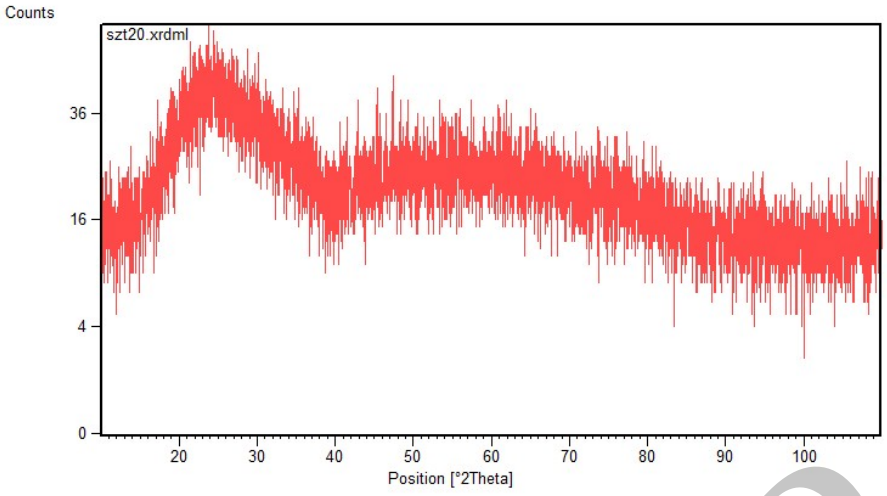

Fig. 8. XRD pattern of polymeric top layer membrane heated at 500 ºC for 1 hour

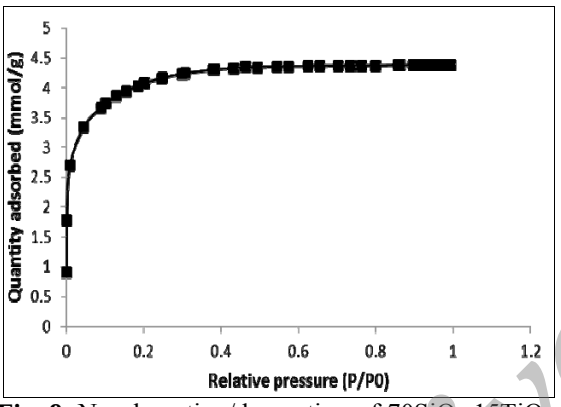

Fig. 9. N_2 adsorption/desorption of $70SiO_2$-$15TiO_2$-$15ZrO_2$ ceramic membrane heated at 500 ºC for 1 hour

interlayer pores was successfully prevented.

3. 4. 2. Structural properties

Fig 8 shows the phase behavior of the top layer material. Initially, the polymeric sol-gel derived ceramic membrane showed a completely amorphous structure. The shape of the adsorption/desorption isotherms was characterized as type I, which confirmed the fine microporous characteristic of this membrane material with mean pore size < 2 nm, surface area 385.14 m^2/g, and pore volume 0.31 cm^3/g (Fig9).

3. 4. 3. Corrosion characteristics

3. 4. 3. 1. Morphology

Fig 10a-c shows the surface of the polymeric top layer before and after corrosion test. As can be seen, an uncorroded membrane showed a distinct top layer, whereas the corroded membrane revealed a surface with non-uniform coverage of the top layer. According to Hofiman-zuter [13], this indicated that membrane corrosion is due to local corrosion effects. It indicates that membrane corrosion is due to local corrosion effects. According to XRD results, the heated ceramic membrane was amorphous. The crystalline materials are more stable than amorphous materials in acid and basic solutions. In this situation, the obtained membrane was deteriorated in corrosion conditions.

3. 4. 3. 2. Phase composition

Phase composition of the ceramic membrane heated at 500 ◦C for 1 hour after corrosion test at different pH is shown in Fig 11. As can be seen, the membrane was amorphous and no crystalline phase was detected. Therefore, the structure of membrane has not been affected by corrosion conditions.

3. 4. 3. 3. Dissolutions into the solutions

Dissolution of Ti, Zr, and Si ions was measured in highly acid and basic solutions after the corrosion test at 25 ºC as shown in Table 3. Dissolution of the ions increased in high acid and basic solutions. The dissolution of elements is controlled by chemical reactions and by diffusion of ions through the product layer [14]. Dissolution of the ions is influenced by the specific surface area and sintering temperature.

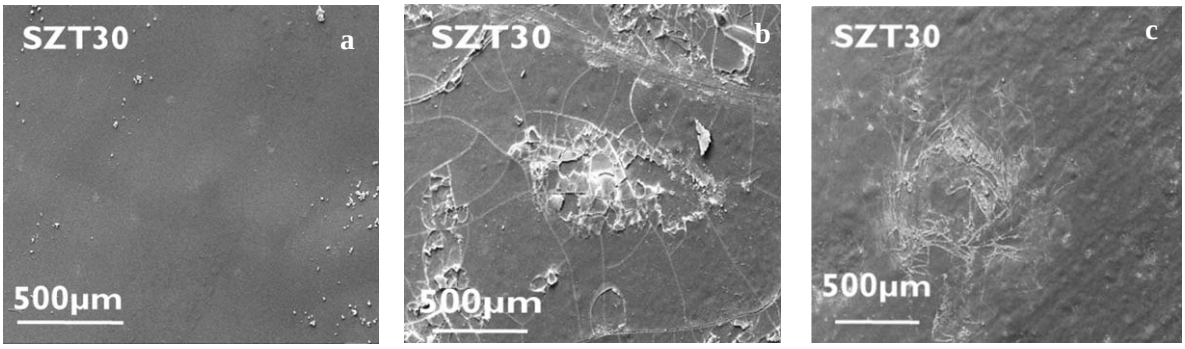

Fig. 10. FESEM surface of the top layer ceramic membrane heated at 500 ºC for 1 hour (a) untreated membrane (b) corroded at pH=3 (c) corroded at pH=11 for 7 days

Table 3. Dissolution of Si, Ti and Zr in acid and basic solutions after corrosion in different pH for 7 days (ppm)

Solution (pH)	Si	Zr	Ti
HNO_3 (1)	0.709	0.178	0.181
HNO_3(3)	0.699	0.124	0.075
NH_4OH (9)	0.678	0.091	0.057
NH_4OH (11)	6.504	-	-

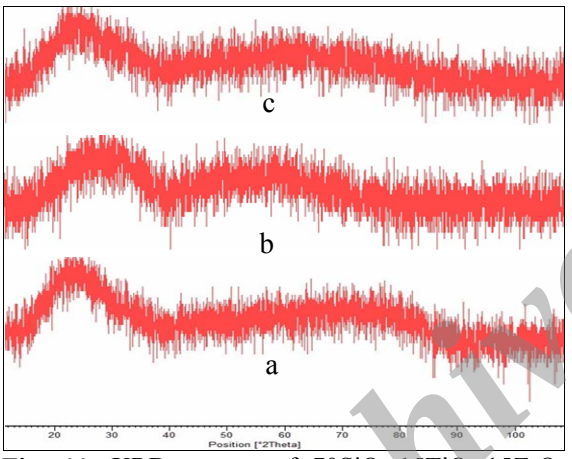

Fig. 11. XRD pattern of $70SiO_2$-$15TiO_2$-$15ZrO_2$ membrane heated at 500 ºC for 1 hr before (a) after corrosion test (b) pH=1 and (c) pH=9 for 7days

The lower the specific surface area and the higher the sintering temperature, the lower is the amount of ions dissolved [15]. In ceramic membrane the dissolution of ions is enhanced as compared to dense components, due to the higher surface area exposed to the media and the lower sintering temperature applied in the processing of membrane. The degree of attack in corrosive media depends partly on thermodynamic properties of reactants and products, but can also be greatly influenced by kinetic effects. A layer of protective product can limit the corrosive attack. In aqueous solutions, hydration of zirconia and titania may take place to form zirconium hydroxides: $ZrO_2.H_2O$, $ZrO_2.2H_2O$ and titanium hydroxides: $TiO_2.H_2O$, $TiO_2.2H_2O$. The solubility of these hydroxides is much lower than that of their oxides [16]. Zr and Ti as base metals, dissolve as Zr^{4+}, ZrO_2^{2+}, Ti^{4+}, TiO_2^{2+} in highly acid solutions and as $HZrO^{3-}$ and $HTiO^{3-}$ in very alkaline solutions [16]. Silica is dissolved as silicate SiO_3^{2-} almost simultaneously in very alkaline solutions.

3. 4. 3. 4. Weight loss

Weight loss of the samples in acid and basic solutions as a function of pH at 25 ºC is shown in Fig 12. Weight loss of the samples increased when pH increased at 25 ºC. The chemical reactions in highly acid and basic solutions caused the detected increase in weight loss. Amorphous silica, which is acid metal oxide, is not stable in aqueous solutions, especially in alkaline solutions. The amount of silica in composition is higher than zirconia and titania (70%wt). Therefore, samples in basic solutions showed lower weight loss than those in acid solutions.

It must be noted that although weight change is a widely used parameter to monitor the corrosion, it has some short comings in this case. It was measured after a certain period, assuming that weight change had a constant rate during corrosion, whereas this seldom

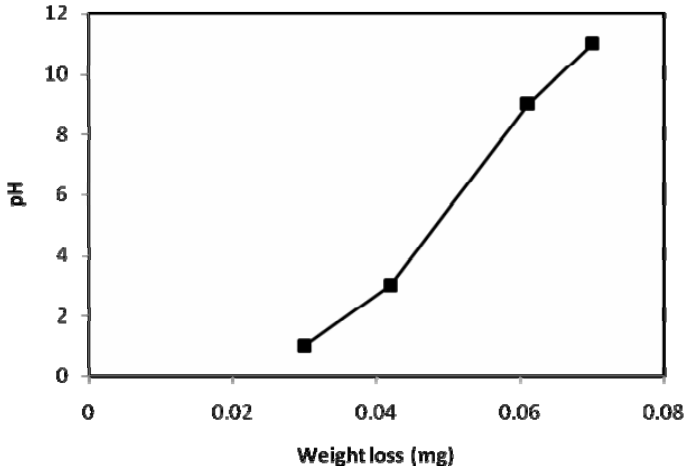

Fig. 12. Weight loss of $70SiO_2$-$15TiO_2$-$15ZrO_2$ membrane in different pH at 25 ºC for 7 days

Table 4. Structural parameter of untreated and corroded $70SiO_2$-$15TiO_2$-$15ZrO_2$ membrane for 7 days

Solution (pH)	Surface (m^2/g)	Pore volume (cm^3/g)	Pore diameter (nm)
Untreated membrane	325.46	0.044	1.8
HNO_3 (1)	234.52	0.065	3.4
HNO_3 (3)	298.12	0.049	2.8
NH_4OH (9)	332.41	0.052	2.5
NH_4OH (11)	354.32	0.058	3.7

happens; and it is common that the rates of attack diminish with time due to the formation of films of corrosion products.

3. 4. 3. 5. Pore size and surface area

Porosity of the samples exposed to acid solutions at pH=1 and 3 and NH_4OH solution at pH=9 and 11, showed an increase to different extent from 1 to about 5% after the corrosion test (Table 4).

The sample in HNO_3/pH=3 showed about 1% increase in porosity. The samples in NH_4OH/pH=11 and in HNO_3/pH=1 showed higher increase in porosity to about 5% after corrosion. The pore size increased as compared to the pore size of the original membrane. The removal of the finest pores was most likely due to the pore closure by corrosion products. Very fine pores are usually intra-agglomerate pores that may fill up readily during corrosion. Specific surface area of the samples in basic solutions showed an increase in surface area. The increase in the surface area arises mostly from the finer portion of pores that have a high area to volume ratio. The filling of the fine pores results in a decrease in surface area in samples exposed to acid solutions. On the other hand, surface area increases in samples after corrosion due to the increase in porosity and surface roughness. The resulting surface area reflects both of these counter-balancing effects.

3. 4. 3. 6. pH of solutions after corrosion test

The change of pH after the corrosion test at 25 ºC is presented in Fig 13. The ionic exchange between the corrosive media and membrane surface in chemical reactions or dissolution results in a change of the pH of solutions. This indicates the extent of reactions which involve H^+ and OH^-, between the solutions and the membrane.

Zirconia and titania are amphoteric in nature, which means that different reactions are dominant in acid and basic solutions. These reactions can be modeled as follows:

$MOH + H^+ \longleftrightarrow MOH_2^+$ [1]

$MOH + OH^- \longleftrightarrow MO^- + H_2O$ [2]

Where the proton is in fact the potential

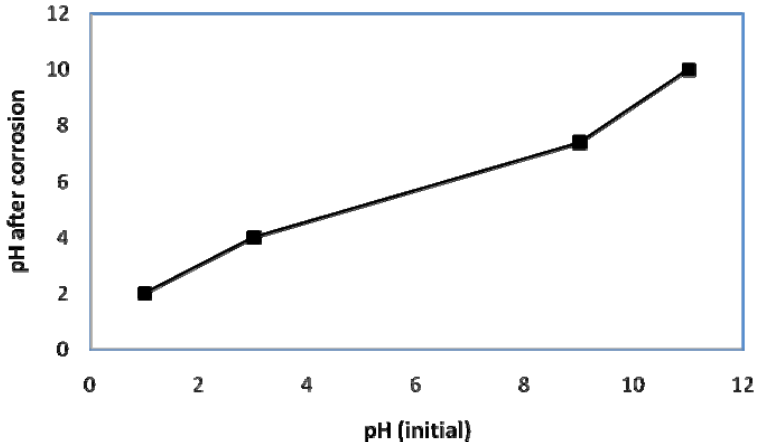

Fig. 13. PH of solution after corrosion of membrane in acid and basic solutions for 7 days

determining ion. Due to the amphoteric nature of the zirconia and titania surface, different types of chemical reactions at each given pH are favored, depending on the net surface charge of the membrane and the ions in the solution. When the concentration of the potential determining ion is altered, the relative adsorption of ions on the surface varies [27]. In acid solutions, the pH after corrosion shifted to higher pH values whereas shifted to the lower pH values in the basic solutions, due to amphoteric reactions of titania and zirconia. It is speculated that at highly acid and basic pH, i.e. pH=2-3 and 11-12 respectively, the ionic density is high and the ionic exchange between the corrosive solutions and the membrane surface is controlled by kinetics of corrosion. At slightly acid and basic pH (5 and 8.5), the corrosive reactions are limited by the number of reactive ions in the solutions and it justifies the lower pH change at this range of pH.

4. Conclusions

In this study, ceramic membrane was obtained using a sol-gel dip coating procedure with mean pore size<2 nm. The corroded membrane showed a non-uniform surface. Phase structure of the membrane was amorphous before and after corrosion test. Dissolution of the ions increased in high acid and basic solutions. Porosity and pore size increased after corrosion test. The pore size increased as compared to the pore size of the original membrane. Surface area of the membrane increased in basic solution, whereas decreased in acid solution. The pH of the solutions showed a shift towards basic pH and in basic solutions a shift towards acid pH.

References

1. T. V. Gestel, H. Kruidhof, H. A. Blank, J. M. Bouwmeester, "ZrO_2 and TiO_2 membranes for nanofiltration and pervaporation Part 1. Preparation and characterization of a corrosion-resistant ZrO_2 nanofiltration membrane with a MWCO < 300", J. Membr. Sci., Vol. 284, 2006, pp. 128-136.
2. R. R. Bhave, Inorganic Membranes: Characterization and Applications, Ph.D. Thesis, University of Twente, Enschede, The Netherlands, 2004.
3. J. M. Hofman-Züter, Chemical and thermal stability of mesoporous ceramic membranes, Ph.D. Thesis, University of Twente, Enschede, The Netherlands, 2001.
4. T. V. Gestel, C. Vandecasteele, Anita Buekenhoudt, "Corrosion properties of alumina and titania NF membranes", J. Membr. Sci., Vol. 214, 2003, pp. 21-29.
5. L. P. Raman, M. Cheryan, N. Rajagopalan, "Consider nanofiltration for membrane separations", Chem. Eng. Progr., Vol. 211, 2001, pp. 83-90.
6. R. Soria, S. Cominotti, "Nanofiltration ceramic membrane", in: Proceedings of the International Conference of Membranes and Membrane Processes, Yokohama, Japan, 18-23 August.
7. R. Vacassy, C. Guizard, V. Thoraval, L. Cot, "Synthesis and characterisation of microporous zirconia powders, Application in nanofiltration characteristics", J. Membr. Sci., Vol. 132, 1997.

8. S. Benfer, U. Popp, H. Richter, C. Siewert, G. Tomandl, "Development and characterization of ceramic nanofiltration membranes", Separat. Purif. Technol., Vol. 22, 2001, pp. 231-237.
9. T. V. Gestel, C. Vandecasteele, Anita Buekenhoudt, Chris Dotremont, "Alumina and titania multilayer membranes for nanofiltration: preparation, characterization and chemical stability", J. Membr. Sci., Vol. 207, 2002, pp. 73-89.
10. A. Larbot, S. Alami-Younssi, M. Persin, J. Sarrazin, L. Cot, "Preparation of α -alumina nanofiltration membrane", J. Membr. Sci., Vol. 97, 1994, pp. 167-173.
11. V. T. Zaspalis, W. Van Praag, K. Keizer, J. R. H. Ross, A. J. Burggraaf, "Synthesis and characterization of primary alumina, titania and binary membranes", J. Mater. Sci., Vol. 27, 1992, pp. 10-23.
12. A. J. Burggraaf, K. Keizer, in: R. R. Bhave, Synthesis of Inorganic membranes, Inorganic membranes: Characterization and Applications, van Nostrand Rheinhold, New York, 1991, pp. 10-63.
13. J. M. Hofman-Züter, Chemical and thermal stability of mesoporous ceramic membranes, Ph.D. Thesis, University of Twente, Enschede, The Netherlands, 1995.
14. M. Shimada, T. Sato, "Corrosion of silicon nitride ceramics in HF and HCl solutions", in: R.E. Tressler, M.McNallan (Eds.), Ceram. Trans., Vol. 10, Am. Creram. Soc., Ohio, 1989, pp. 355.
15. J. C. Farinas, R. Moreno, J. Requena, "Acid-basic stability of Y-TZP ceramics", Mater. Sci. Eng.,Vol. 109, 1989, pp. 97-99.
16. M. Pourbaix, "Atlas of electrochemical equilibriuia in aqueous solutions", NACE celebcor, 1974, pp. 223-229.